

## 2006 North Sea Sand Ripple Formation by Currents

GENERAL OVERVIEW	
<b>Dataset name:</b> <i>Occurrence of current-induced active sand ripples at the sea floor of the North Sea for the year 2006</i>	
<b>Project:</b> <i>North Sea – Observation and Assessment of Habitats (NOAH)</i>	
<b>Co-Principal Investigator:</b> <i>Walter Puls , Ulrike Kleeberg (Metadata and Web Services) , Dietmar Sauer (Model Tool)</i>	
<b>Contact:</b> <i>Helmholtz-Zentrum Geesthacht (HZG), Max-Planck-Straße 1, 21502 Geesthacht, Ulrike.Kleeberg@hzg.de</i>	
DATASET SPECIFICATIONS	
<b>Dataset Parameter(s) and supplied Unit(s):</b> <i>Time percentage of active current ripple</i>	
<b>Date(s) available:</b> <i>2006, Model Tool (1984 – 2015, , resolution hourly)</i>	
<b>Validated:</b> <i>See Notes and Limitations</i>	<b>Version Date:</b> <i>14.03.2007</i>
<b>Current State:</b> <i>Updates expected</i>	
<b>Format:</b> <i>netCDF, Vector (Esri FGDB), CSV</i>	
<b>Citation:</b>  <i>Kapitza H. and D. Eppel (2000). " Simulating morphodynamical processes on a parallel system". In: Spaulding ML and Butler HL (eds) Estuarine and Coastal Modelling, Proceedings of the sixth International Conference. New Orleans, Louisiana, USA, November 3-5, 1999</i>  <i>Marten, K.V., (2010). " Field Observation and Modelling of Near-shore Sediment Transport Processes". Ph.D. Thesis. School of Ocean Sciences, Bangor University, UK.</i>  <i>Pätsch, J., H. Burchard, C. Dieterich, U. Gräwe, M. Gröger, M. Mathis, H. Kapitza, M. Bersch, A. Moll, T. Pohlmann, J. Su, H. T. M. Ho-Hagemann, A. Schulz, A. Elizalde and C. Eden (2017). "An evaluation of the North Sea circulation in global and regional models relevant for ecosystem simulations." Ocean Modelling 116: 70-95.</i>  <i>Pohlmann, T., Puls, W., 1994. Currents and transport in water. In: Sündermann, J. (Ed.), Circulation and Contaminant Fluxes in the North Sea. Springer Berlin Heidelberg, Berlin, Heidelberg, pp. 345–402</i>  <i>Soulsby, R., 1997. Dynamics of Marine Sands: A Manual for Practical Applications.</i>	



Thomas Telford Ltd, London.

Soulsby, R.L., Whitehouse, R.J.S., (2005a). "Prediction of Ripple Properties in Shelf Seas. Mark 1 Predictor"., Report TR150, HR Wallingford, Wallingford, UK.

<http://eprints.hrwallingford.co.uk/280/> accessed February 2012).

Soulsby, R.L., Whitehouse, R.J.S., (2005b). "Prediction of Ripple Properties in Shelf Seas. Mark 2 Predictor"., Report TR154, HR Wallingford, Wallingford, UK.

<http://eprints.hrwallingford.co.uk/281/> accessed February 2012).

Weisse, R., and H. Günther (2007), Wave climate and long-term changes for the Southern North Sea obtained from a high-resolution hindcast 1958–2002, *Ocean Dyn.*, 57, 161–172,

<https://doi.org/10.1007/s10236-006-0094-x>.

## DATASET DETAILS

### Abstract

Hydrodynamic model output was used to map the frequency of occurrence of current-induced active sand ripples at the sea floor of the southern North Sea for the year 2006. Formation and persistence of active ripples have a meaning for advective flow within the sediment and thus the ventilation of pore water with oxygen.

The map shows the time percentage of active current-generated ripples (calculated by the ripple predictor of c) during 2006 in the southern North Sea.

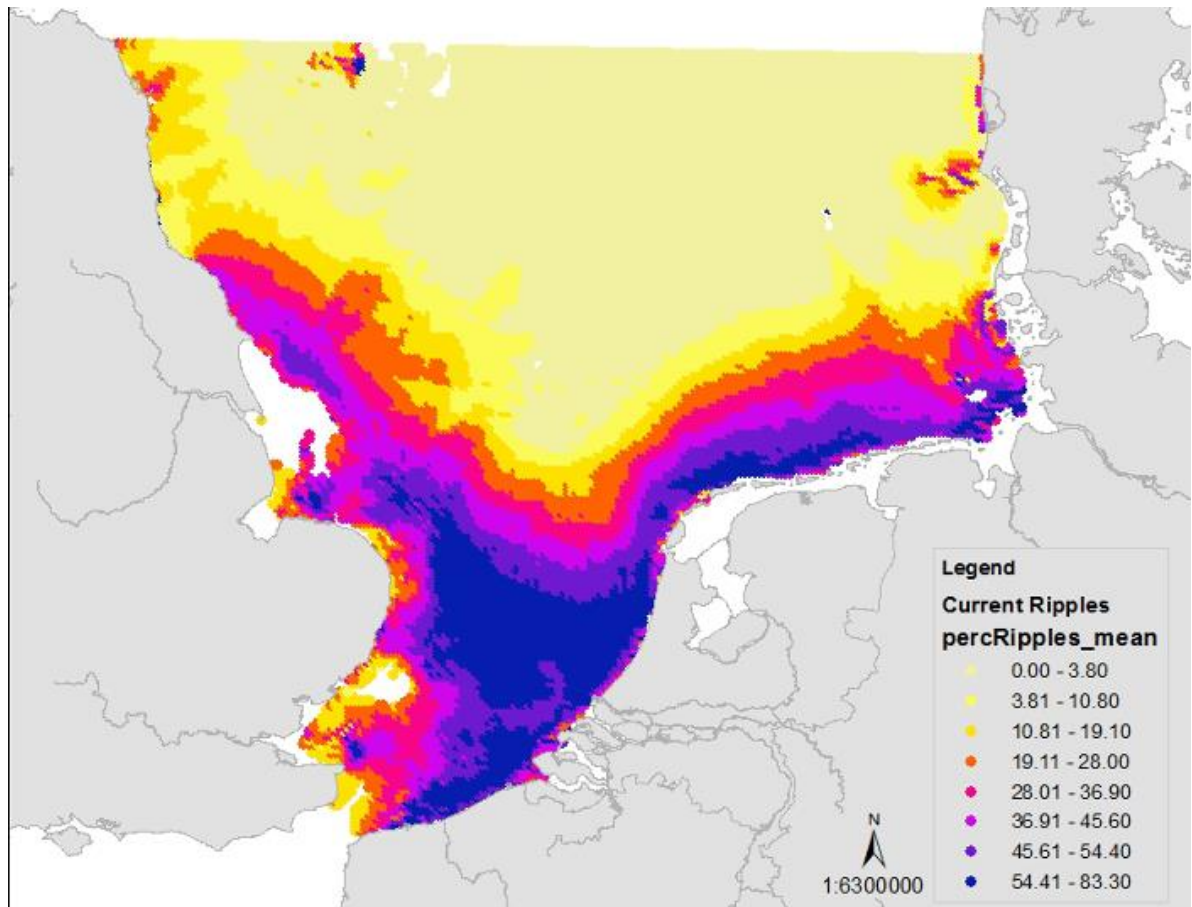
Current-generated ripples are called "active" if (a) near-bed currents generate sediment transport at the sea floor (i.e. if the current bed shear stress  $\tau_c$  is above the threshold of sediment motion), and if (b) the bed shear stress  $\tau_c$  produced by currents is above a certain value of the bed shear stress  $\tau_w$  produced by waves. The latter point (b) is a simplifying description of the "wave-current dominance criterion" given in Marten (2010). In contrast to "active current ripples", so-called "frozen current ripples" exist during times when the near-bed current is too weak to induce sediment transport. During such times ripples remain as they are, unless they are not degraded (flattened) by activities of benthic animals.

The characteristics of current-generated ripples are: As soon as the current skin-friction shear stress  $\tau_c$  exceeds the value  $\tau_{CR}$  required for sediment movement, the bed is molded into a series of small asymmetrical bedforms called current ripples. Current-generated ripples migrate slowly in the direction of the current. Viewed from above, current-generated ripples form an irregular, strongly three-dimensional pattern. Ripples only form in sand with grain-sizes between  $\approx 60 \mu\text{m}$  and  $\approx 800 \mu\text{m}$ . The length of current-generated ripples is typically 1000 times the median grain-size. The height of "fully developed" current-generated ripples is a few centimeters only: for current ripples it is  $\approx 0.1$  times the ripple wave length.

Current-generated ripples exist as long as the near-bed current shear stress is below the threshold for so-called sheet flow (plane bed with intense sediment transport). As an example: For a median grain-size of  $200 \mu\text{m}$ , sheet flow is expected for near-bed current velocity (average of the bottom few meters) of  $> 1 \text{ m/s}$ .

The percentage of "active current ripple existence" in the southern North Sea shows highest values in the areas with strong (tidal) currents. The median grain-size is above  $800 \mu\text{m}$  in the area off Humber which prevents the development of ripples. Off East Anglia and off Thames mouth, the grain-size of bottom sediment is so coarse that ripples only develop at times of highest current speeds. Active current-generated ripples do not exist during times when (a) the bed shear stress

due to wave action  $\tau_w$  is somewhat greater than  $\tau_c$  or (b)  $\tau_c$  is below the threshold of sediment motion or (c)  $\tau_c$  is above the threshold for sheet flow.



### Acquisition and Processing Description:

#### Acquisition:

The requirements for current-generated ripple prediction are the availability of: (1) the bed shear stresses generated by waves and currents (including their directions) and (2) the median grain-size of bottom sediments.

The bed shear stress  $\tau_w$  produced by waves is calculated from results of the WAM model while the bed shear stress  $\tau_c$  produced by currents is calculated from results of the TRIM model. Both models are used for long-term computation runs (several years) at the Institute of Coastal Research, HZG Geesthacht. Both  $\tau_c$  and  $\tau_w$  are provided as gridded, area-covering data.

The basis for the median grain-size distribution consists of more than 50,000 individual samples. Only samples from the sediment surface (maximum sub-bottom depth 10 cm) were taken into account. The grain-size data were collected from more than 10 institutions and databases. A full-coverage gridded estimation of the median grain-size is obtained by Co-Kriging.

#### Processing Description:

The prediction of ripples in the North Sea uses the formulas and prescriptions of Soulsby and Whitehouse (2005), supplemented by Marten (2010). Their model predicts the existence, the type (current-generated or wave-generated) and the height, length and orientation of sand ripples. The model includes processes as threshold of motion, ripple wash-out and biological degradation.

The requirements for applying the ripple predictor are the availability of: (1) the bed shear stresses generated by waves and currents (including their directions) and (2) the median grain-size. Concerning biological degradation of ripple height during times of “sediment movement = 0”, Soulsby and Whitehouse (2005) use a mean lifetime of 72 hours (i.e. after 72 hours the ripple height is reduced to 1/e times the initial height). The uncertainty about the mean lifetime is huge. In the ripple predictor the same current-generated bed shear stress  $\tau_c$  was used as given in the appropriate map. The applied wave-generated bed shear stress  $\tau_w$ , however, is different from the conventional  $\tau_w$ . In the ripple predictor the amplitude of the wave orbital velocity just above the bed,  $U_w$ , is represented by  $U_{1/10}$ , the mean of the highest one-tenth velocities generated by natural (random) waves. For the calculation of  $U_{1/10}$ , the significant wave height  $H_s$  and the mean wave period  $T_{m2}$  were converted to  $H_{1/10} = 1.27 \cdot H_s$  and  $T_{1/10} = 1.28 \cdot T_{m2}$ . The amplitude of the wave skin-friction shear-stress  $\tau_w$  is then calculated by the standard formula

$$\tau_w = \frac{1}{2} \cdot \rho_w \cdot f_w \cdot U_{1/10}^2$$

where  $f_w$  is the wave friction factor and  $\rho_w$  is the density of sea water.

In simplified terms, there are four seabed conditions predicted by the model:

(1) “active” wave ripples exist if the wave bed shear stress  $\tau_w$  is above the threshold of sediment motion, and if

$$\theta'_w \geq \max(0.42 \cdot \theta'_c^{0.47}, 0.04)$$

with  $\theta'_w$  and  $\theta'_c$  being the skin friction wave Shields parameter and the skin friction current Shields parameter, respectively.

(2) “active” current ripples exist if the current bed shear stress  $\tau_c$  is above the threshold of sediment motion, and if

$$\theta'_w < \max(0.42 \cdot \theta'_c^{0.47}, 0.04)$$

(3) “frozen” (or “relict”) ripples exist if both  $\tau_c$  and  $\tau_w$  are below the threshold of motion. The previous ripples remain as they are, unless biological activity flattens them.

(4) For large  $\tau_c$  ripples are washed out, leaving a flat bed (sheet flow)

To produce an area-covering map of “time percentage of current-generated ripples during 2006” the first step was the generation of area-covering maps of  $\tau_c$ ,  $\tau_w$  and median grain-size. Concerning  $\tau_c$  and  $\tau_w$ , the models TRIM and WAM yield area covering current and wave data from which  $\tau_c$  and  $\tau_w$  are determined. For the year 2006 these maps of  $\tau_c$  and  $\tau_w$  are provided with a time step of one hour. Concerning the median grain-size, a map was produced by spatial interpolation of individual sample data. This interpolation was done by Co-Kriging using the R-routine “krige” (R-library “gstat”). The external variable used by Co-Kriging was log-converted %mud.

For every full hour during 2006, a map “frequency of active current ripples” was produced from the median grain-size and the full hour values of  $\tau_c$  and  $\tau_w$ . The final step was to generate a map “frequency of current-generated ripples” for the whole year 2006.

## Notes and Limitations:

Data Quality:



Concerning the quality of the input data of the ripple predictor of Soulsby and Whitehouse (2005) see the quality assessments of the bed shear stress generated by currents, of the bed shear stress generated by waves and of the median grain-size.

Concerning the quality of the map “frequency of current-generated ripples during 2006”, three aspects are discussed:

The first quality aspect concerns the wave-current dominance criterion of the ripple predictor: it is assumed that there exist either current-only or wave-only ripples. In Soulsby et al. (2012) it is argued that the assumption “only one ripple train is present at any time” has been made for simplicity of modelling. In reality “ripples can occur as two overlapping trains, one due to waves and one due to currents

The second quality aspect concerns the threshold of sediment motion. The used threshold formula is that of Shields (Soulsby 1997). The sediment of shelf seas, however, may be armored to some extent. Sediment armoring increases  $\tau_{CR}$ , the threshold bed shear stress for sediment motion. As an example: for a median grain-size of 200  $\mu\text{m}$ ,  $\tau_{CR}$  given by the Shields formula is 0.15  $\text{N m}^{-2}$ . Compared to this, Pohlmann and Puls (1994) observed an erosion threshold shear stress in the German Bight (sandy sediment) of  $\tau_{CR} \approx 0.8 \text{ N m}^{-2}$ . An increase of  $\tau_{CR}$  would appreciably reduce the “existence time of active current ripples”.

The third quality aspect concerns the exclusion of frozen current-generated ripples in the map. The effect of ripples, e.g. on the transport of nutrients and oxygen in the sediment bed, is independent of the ripple status “active” or “frozen”. By showing only the frequency of active ripple existence, the map gives a skewed impression of ripple existence. The reason why existence times of frozen ripples were not included in the map was: the existence time of frozen ripples is extremely uncertain because little is known about the speed of ripple degradation (flattening) by benthic animals.

#### Error Estimation:

The existence of a certain type of bedform depends on the hydrodynamic and the sedimentary conditions. “Current ripples” may be predicted at a particular site and a particular time, but this prediction is uncertain if hydrodynamic and sedimentary input data contain some degree of uncertainty.

The uncertainty of one predicted classification as “current ripples” depends on the uncertainties of the input data and of the prediction formulas used for the classification. These uncertainties (given as standard deviations) are:

(1) The uncertainty of the median grain-size  $D_{50}$ . The uncertainty in  $\phi$ -scale is about  $\pm 0.68$ . This uncertainty is the Kriging standard deviation shown here.

(2) The uncertainty of the near-bed current velocity which is estimated to be  $\pm 14 \%$ .

(3) The uncertainty of the two wave parameters used for the calculation of the near-bed amplitude  $UW$  of the wave orbital velocity: the wave height and the wave period. Weisse and Günther (2007) report on a comparison between observed and hindcast wave data in the North Sea. The relative errors of the significant wave height  $H_S$  and the mean wave period  $T_{m2}$  were found to be  $\pm 30 \%$  and  $18 \%$ , respectively. The wave parameters are needed (together with the current data) to decide whether there are wave ripples, current ripples or neither of the two ripple types.

(5) The uncertainty of the calculated wave (skin-) friction factor  $f_W$ . The uncertainty of the wave friction factor is estimated from the data points plotted in Fig. 15 (Soulsby 1997). The plot shows the deviations of a fitted  $f_W$ -equation from measured  $f_W$  data. The standard deviation of the difference between fitted  $\log(f_W)$  and measured  $\log(f_W)$  is  $\pm 0.11$ .



(6) The uncertainty of the criterion which groups the ripples into wave dominated and current dominated ripples. The uncertainty of the criterion (the uncertainty if all input data are precisely known) was deduced from Fig. 5.21 in Marten (2010). This scatterplot shows a stability diagram to define the bounds of the current dominated and wave dominated bedform regimes. The criterion for wave/current dominance at the bed is given in the text about Data Processing. The uncertainty of the criterion is represented by an uncertainty of  $\pm 0.05$  for  $\log \vartheta'W$ . Here  $\vartheta'W$  is the value of the skin friction wave Shields parameter separating between current dominated and wave dominated ripples.

The uncertainty of the predicted classification as “current ripples” is composed of the uncertainties given above. The uncertainties are joined by a Monte Carlo procedure. The random numbers for the Monte Carlo procedure were taken from a normal (Gaussian) distribution. Typically  $N = 10000$  realizations of “bedform type” were calculated during a Monte Carlo simulation run for one error estimation.

The uncertainty of being classified as “current ripples” depends on the impact of waves. If waves play a major role, current ripples can only exist in the window between “ $\tau C$  somewhat larger than  $\tau W$ ” and “begin of sheet flow”. Such conditions, however, are rare in the southern North Sea and are thus not considered here.

If waves play a minor role, current ripples exist in the window between “threshold of sediment movement ( $\tau C > \tau CR$ )” and “begin of sheet flow”. This window is rather large. In the middle of this window the prediction “current ripples” has a small uncertainty. This is particularly the case in the central and the southern part of the Southern Bight where waves play a minor role in generating ripples and where the frequency of current ripples is above 60 %. At the window’s edges, however, the prediction “active current ripples” is only correct in about 50 % of all Monte Carlo realizations.

An example for the upper edge of the window is the English coast where tidal current velocities become high enough to flatten the bed.

An example for the lower window edge is the broad transition zone (from Yorkshire to the German Bight) between 50 % and 20 % active current ripple occurrence in the south and the north, respectively. Within a tidal cycle, currents which are strong enough ( $\tau C > \tau CR$ ) to generate sediment transport (and thus to form current ripples) alternate with currents which are below the threshold of sediment movement ( $\tau C < \tau CR$ ). It may be argued, however, that the distinction between “active current ripples during times of  $\tau C > \tau CR$ ” and “frozen ripples during times of  $\tau C < \tau CR$ ” is rather far-fetched. The time between two periods with active ripples is a few hours only. It can be assumed that the ripples in their frozen state will not be flattened considerably within these few hours. This means that the prediction “active current ripples” should be replaced by the prediction “current ripples, both active and frozen”. The uncertainty of this prediction is then very small.

#### Instruments/Models:

The prediction of ripples in the North Sea uses the formulas and prescriptions of Soulsby and Whitehouse (2005). Their model predicts the existence, the type (current- or wave-generated) and the height, length and orientation of sand ripples. The model includes processes as threshold of motion, ripple wash-out and biological degradation.

#### Related Datasets:

- Median grain-size of the surface sediment grain-size distribution
- Bed shear stress generated by currents
- Bed shear stress generated by waves

- *Heights of active wave-generated ripples*

### Data Sources

The data for the generation of sediment maps were obtained from the following institutions:

#### **NAVAL OFFICES and RESEARCH INSTITUTES:**

Forschungs- und Technologiezentrum Büsum, Germany  
Bundesamt für Seeschifffahrt und Hydrographie (BSH), Hamburg, Germany  
Senckenberg Institut Wilhelmshaven, Germany  
Helmholtz Zentrum Geesthacht, Germany  
Bioconsult Schuchardt & Scholle GbR, Bremen, Germany  
Deltares, Utrecht, The Netherlands  
British Geological Survey, Marine Information Project, Edinburgh, UK  
Marine Scotland, Marine Laboratory, Aberdeen, UK  
Universität Hamburg, Institut für Geologie und Paläontologie, Hamburg, Germany  
Royal Netherlands Institute for Sea Research (NIOZ), Texel, The Netherlands  
Geological Survey of the Netherlands (TNO), Utrecht, The Netherlands  
School of Ocean Sciences, Bangor University, Menai Bridge, Anglesey, UK  
CEFAS, Lowestoft, UK  
Geological Survey of Norway (NGU), Trondheim, Norway  
Geological Survey of Denmark and Greenland (GEUS), Copenhagen, Denmark  
Bureau de Recherches Géologiques et Minières (brgm), Orléans, France

#### **PROJECTS:**

Management, Research and Budgeting of Aggregates in Shelf Seas related to End-users (MAREBASSE, 2002-2006), Ghent University, Belgium  
North Sea Benthos Survey 1987  
North Sea Benthos Project 2000  
Zirkulation und Schadstoffumsatz in der Nordsee (ZISCH, 1984-1989), Universität Hamburg  
Biogeochemistry and Distribution of Suspended Matter in the North Sea and Implications to Fisheries Biology (TOSCH, 1984-1988), Universität Hamburg  
Geopotenzial Deutsche Nordsee (GPDN, 2009-2013), Bundesanstalt für Geowissenschaften und Rohstoffe (BGR) Hannover, Landesamt für Bergbau, Energie und Geologie (LBEG) Hannover, Bundesamt für Seeschifffahrt und Hydrographie (BSH) Hamburg, Germany

#### **DATABASES:**

Flanders Marine Institute (VLIZ) Data Centre, Ostend, Belgium  
Management Unit of the North Sea Mathematical Models (MUMM), Brussels, Belgium  
International Council for the Exploration of the Sea (ICES), Copenhagen, Denmark  
Publishing Network for Geoscientific & Environmental Data (PANGAEA), Alfred-Wegener-Intitut (AWI), Bremerhaven, Germany